Cryst. Latt. Def. and Amorph. Mat.,
1985, Vol. 12, pp. 381-400
0732-8699/85/1204-0381$18.50/0

ESR, ENDOR AND ODMR OF COLOR CENTERS AND OTHER DEFECTS IN IONIC CRYSTALS

J.-M. SPAETH
Fachbereich Physik, University of Paderborn,
Warburger Str. 100 A, D-4790 Paderborn, FRG

Abstract Recent developments in the use of multiple resonance techniques to the determination of the structure of point defects in insulating crystals are briefly reviewed. Computer assisted electron nuclear double resonance (ENDOR) is applied to the investigation of off-center Ni^+ centers in CaF_2 and $F_H(F^-)$ centers in KCl. It was established that in $F_H(F^-)$ centers the F^- ions occupy the fourth shell. The basic ideas of DOUBLE ENDOR are described and their application to the investigation of two types of F-centers in BaFCl and O^- centers in α-Al_2O_3 is presented. Recent experiments with the optical detection of electron spin resonance (ODESR) via the magnetic circular dichroism of the absorption on laser active Tl centers in alkali halides ($Tl^0(1)$ centers) are reviewed and the structure determination of $Tl_2^0(1)$ centers is presented. Finally, first ODENDOR experiments on the antisite defects in GaAs are presented, in which the ligand hyperfine structure could be resolved with this technique.

1. INTRODUCTION

The title of this short review seems all-comprehensive, however, it cannot be attempted within a few pages to cover the whole field of magnetic resonance of defects in ionic crystals. Therefore, it is attempted to show new developments in the experimental methods and their use to determine the structure of defects and to determine directly the correlation of optical and structural properties of defects. The use of advanced electron nuclear double resonance (ENDOR) techniques and the application of optical detection of ESR and ENDOR will briefly be reviewed. The examples chosen are taken from recent work of the Paderborn group, to a great deal not yet

published. All work was performed since the last International Conference on Color Centers in Riga 1981.

2. ELECTRON NUCLEAR DOUBLE RESONANCE (ENDOR)

As is well known since the early work of Feher[1] and Seidel[2], ENDOR can be used to resolve superhyperfine (shf) (ligand hyperfine) interactions much better than ESR and it is the measurement of the shf interactions with nearest and next nearest neighbors and their symmetries which enable the determination of a defect structure. Most widely used is the stationary ENDOR method[2], in which by means of a rf transition between nuclear Zeeman levels the (partial) saturation of the ESR signal is changed. The change in ESR saturation is measured as the ENDOR signal and thus the occurrence of NMR transitions of neighbor nuclei coupled to the paramagnetic electron of the defect is measured. This indirect method is several orders of magnitude more sensitive than a direct NMR observation. For the structure determination the angular dependence of these ENDOR transitions must be measured in order to identify the neighbor nuclei by their symmetry with respect to the center. In ionic crystals the best known example is probably the ENDOR investigation of the F center[2]. A summary of ENDOR results of color centers in alkali halides is given in[3].

I became, however, soon clear, that in most practical cases of interest the angular dependencies of the ENDOR spectra are very complicated, especially in low symmetry defects. There are often cases, where for each crystal orientation several hundred ENDOR lines are measured, as for instance in GaP containing Ni^{3+} centers[4]. In order to follow the angular dependence of a particular ENDOR line, which is necessary for the analysis, one has to measure angular variations in very small steps, a rather tedious task. Therefore, considerable progress was achieved by building a computer controlled ENDOR spectrometer. The computer controls the rf frequency, the magnetic field, the temperature, the cavity matching

and the crystal orientation. This enables automatic measurements of the angular dependencies, of the temperature dependence, and it enables multiple scans if the signal-to-noise ratio is bad, and it also is of invaluable help to have the data in the computer for their analysis. Meanwhile a rather large software packet was developed for the analysis of the ENDOR spectra including the application of digital filters, the automatic determination of the frequency position of the ENDOR lines as well as deconvolution programmes to enhance the resolution[5].

A recent example of an ENDOR investigation is that of Ni^+ centers in CaF_2. It was concluded from ESR measurements that Ni^+ does not reside at the Ca^{++} site, but nearly in a plane spanned by $4F^-$ ions[6] (see Fig. 1).

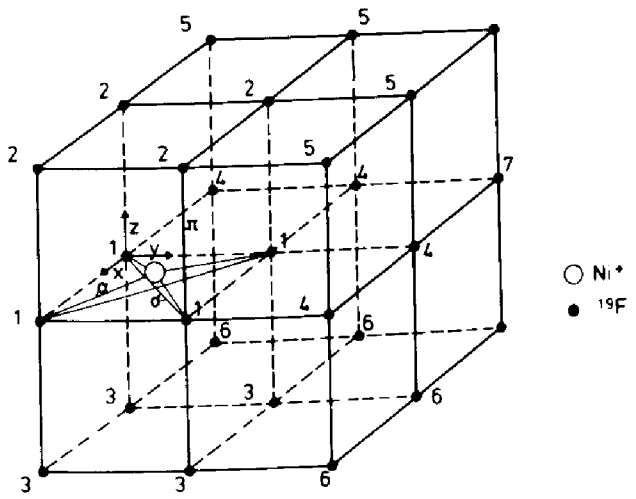

FIGURE 1 Model of Ni^+ centers in CaF_2. The numbers of the nuclear sites denote the shell number. After (7).

With ENDOR the proposed model was to be checked. Fig. 2 shows the angular dependence of the ENDOR spectrum for rotation of the magnetic field in the x-y plane of Fig. 1((!00) plane)). The "dots" are the experimental ENDOR frequencies as plotted from the computer after the end of the experiments. The drawn lines are the theoretical angular dependencies drawn after the analysis of the spectrum with the principal values and orientations of the shf tensors[7]. Inspection of the angular dependence shows, that the "patterns" denoted by 2 and 3 in Fig. 2 are very similar, but not

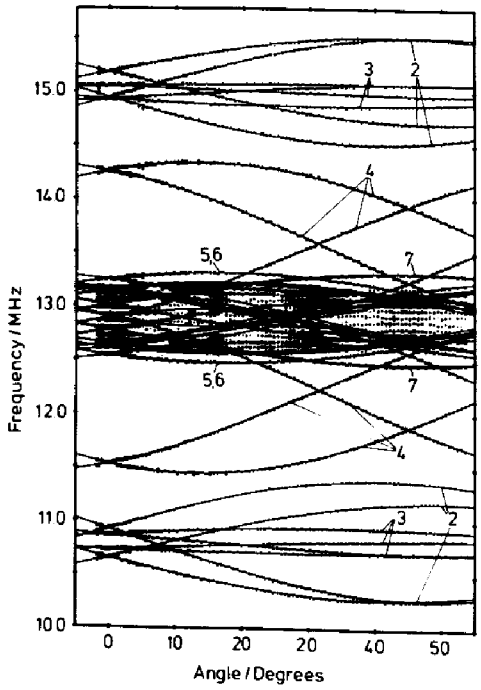

FIGURE 2

Angular dependence of Ni^+ centers in CaF_2 for rotation of the magnetic field in the x-y plane of Fig. 1. $0^o \triangleq [100]$. The dots are the experimental ENDOR frequencies. The drawn curves were calculated with the appropriate spin Hamiltonian. After (7).

identical. The general shape is typical for nuclei of shells 2 or 3 (see Fig. 1) with an axis of the shf tensors pointing approximately to the face center in the face formed by nuclei of shell 1. The fact, that there are two different angular dependencies of this shape shows immediately, that the Ni^+ is not entirely in the plane spanned by the $4F^-$, but somewhat above it. Therefore, the symmetry character of the nuclei of shells 2 and 3 is very similar, but the interactions are somewhat different, since they have different distances from the Ni^+. Altogether, 7 neighbor shells could be accurately analysed. The model proposed from ESR could be confirmed. The striking feature of the results is, however, that except for the nearest neighbors at the nuclei of shells 2 to 7 a negative spin density is found. The isotropic shf constant a (Fermi contact term) is negative, and the anisotropic shf constant b is smaller than the value expected from a classical point dipole-dipole interaction. In reference 7 an explanation is offered for these findings in terms of a transferred exchange polarization, in which the spin paired orbitals of the nearest F^- ions are spin

polarized by the unpaired p-orbital at this F^-, which gives rise to the anisotropic shf constant of the nearest neighbors and which is largely due to a covalency between the Ni^+ 3d electron and its nearest F^- neighbors. The spin polarization is then transferred via ion overlap to the outer shells 2-7. The fact that this effect is so clearly apparent, is due to the special "geometry" of this off-center defect. The described investigation is the first ENDOR study of an off-center defect in an ionic crystal.

ENDOR can also be used to study a photochemical reaction. As was shown earlier by Pan and Lüty[8], F centers can be associated to foreign anions like H^- in alkali halides by bleaching the F-centers at the appropriate temperature of about -40 °C, for instance in KCl doped with H^- ions. It was concluded from the symmetry of Raman lines, that F_H-centers are formed, in which H^- is in a (110) position with respect to the F electron, that is in the second shell. In KCl doped with F^- upon appropriate F-band bleaching a new F-type band is created which is shifted by approximately 0.1 eV to lower energy[9]. The F-center conversion appears to be about 50%. Fig. 3 shows part of the ENDOR spectrum of a sample before F to F_H conversion in the lower trace[6]. The ENDOR lines are due to second shell Cl neighbors. After conversion of about

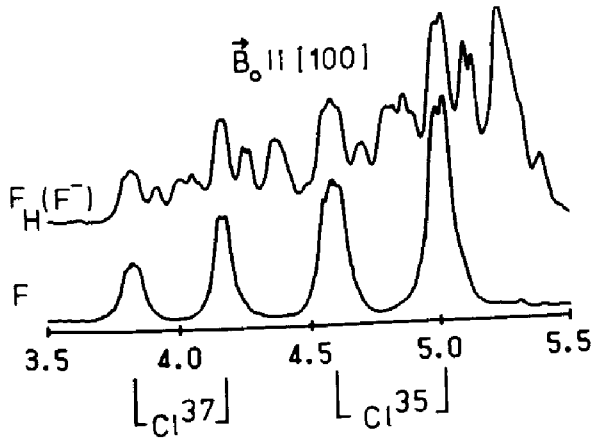

FIGURE 3 Part of the ENDOR spectrum of F and $F_H(F^-)$ centers in KCl. T = 140 K. After (10).
a) Second shell Cl neighbors of F and F_H centers after an approximate 50% conversion of F into F_H centers.
b) Second shell Cl neighbors of F centers.

50% of the F-centers into F_H centers, the ENDOR spectrum contains many new lines (upper trace, Fig. 3a) in addition to the F center lines. The analysis shows that the second shell Cl neighbors are not equivalent anymore, nor are the nearest K neighbors. A search for second shell F^- nuclei, which would have an angular dependence with (110) symmetry, failed. However ^{19}F lines were found with (100) symmetry between 15.2 and 16.3 MHz. The F^- ions occupy (200) positions, that is they are in the 4th shell. In Table 1 the isotropic shf constants of the nearest K neighbors and the 4th shell F^- and Cl^- ions, respectively, of F and F_H centers in KCl are collected.

TABLE 1 Isotropic shf constants of F and $F_H(F^-)$ centers in KCl (in MHz) (T = 80 K) after (10)

nuclei	F centers	$F_H(F^-)$ centers	
K^I	20.7	K_1^I	21.6
		K_2^I	22.1
		K_3^I	12.1
Cl^{IV}	1.1	F^{IV}	4.5

The fact that F^- resides in shell IV follows not only from the (100) symmetry, but also from the number of inequivalent 1st and 2nd shell neighbors as well as from a theoretical estimate of the shf constants. There is no doubt about this assignment. The low isotropic constant of K_3^I is explained by assuming that this nearest K neighbor is moved outward by 12%, while the F^{IV} value indicates an inward distortion of about 4%. Fig. 4 shows a schematic sketch of the resulting center model. The increased space available for the K_3^I and F^{IV} nuclei is also reflected in an unusual temperature dependence of the ENDOR lines. Fig. 5 shows the relative increase

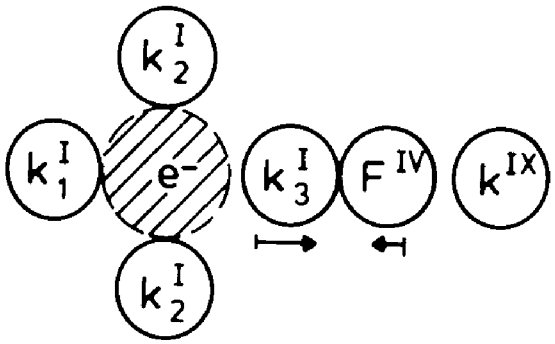

FIGURE 4 Model of $F_H(F^-)$ centers in KCl:F.

of the isotropic shf constant as a function of temperature for the F center (K^I, Cl^{IV}) and the F_H center (K_3^I, F^{IV}). The strong increase of a (K_3^I) compared to the nearest K^I neighbor of the F center and also to the other two K neighbors K_2^I, K_1^I, which have a behavior very similar to that of K^I of the F center, shows that K_3^I moves in a strongly unharmonic potential. With increasing temperature K_3^I gets nearer to the center electron, whereas F^{IV} moves in an unharmonic potential where the unharmonicity is reversed with respect to the (100) direction - it moves further away with increasing temperature. For more detailed discussions see[11]. The results obtained for the $F_H(F^-)$ centers in KCl do not agree with the results of Pan and Lüty on $F_H(H^-)$ centers[8]. A preliminary ENDOR investigation of $F_H(H^-)$ centers in KCl highly doped with H^- ($\sim 5 \cdot 10^{18}$ cm^3), however, showed also only H^- ions with (100) symmetry. An estimate of the magnitude of the H^- shf interaction using the same wave function for the F center as above for the $F_H(F^-)$ center yielded, on the other hand, that the H^- cannot be assumed to reside in the 4th shell. H^- is probably basically in the second shell, but moved towards the center of the vacancy and performing a rapid reorientation motion about a [100] axis, which may be singled out due to another H^- in the 4th shell. This is not unlikely due to the very high H^- concentration. However, more measurements are needed to clarify this point.

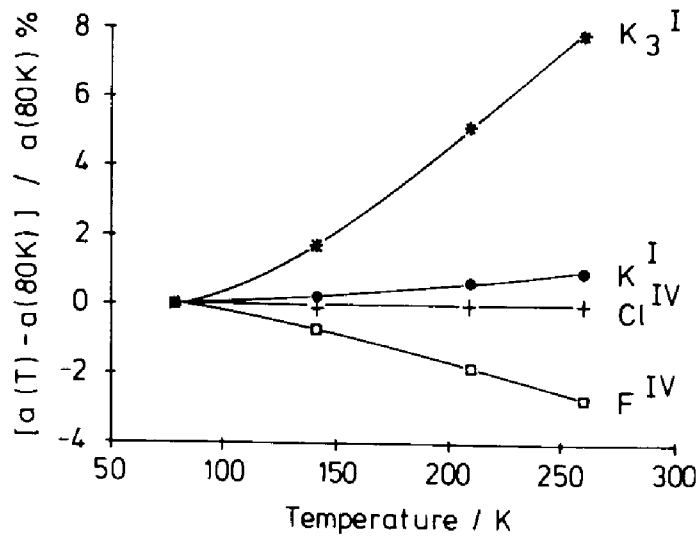

FIGURE 5 Temperature dependence of the isotropic shf constants of nearest potassium (K^I) and 4th shell Cl (Cl^{IV}) neighbors of F centers in KCl and of nearest potassium (K_1^I, K_2^I and K_3^I) and the 4th shell F neighbour of $F_H(F^-)$ centers in KCl. After (10).

3. DOUBLE ENDOR

In an ENDOR experiment the rf induced nuclear magnetic resonance (NMR) transition between the nuclear Zeeman levels of a neighbor nucleus coupled to the unpaired electron by a shf interaction changes somewhat the polarization of the electron spin in the partially saturated situation. This coupling between neighbor nucleus and unpaired electron is indicated schematically by "springs" in Fig. 6. If simultaneously a second NMR transition is induced with a second radio frequency at a nucleus coupled to the same unpaired electron, then the induced change of the electron spin polarization is different from what it would be if the first NMR transition would not occur simultaneously. Thus the polarization change due to the second NMR transition is dependent on the occurrence of the first NMR transition. The total electron desaturation (ENDOR effect) is a function of the product of the effect of the

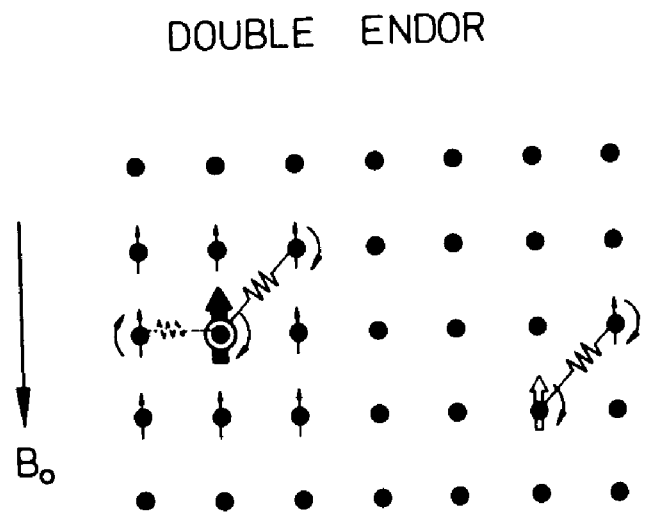

FIGURE 6 Schematic representation of ENDOR and DOUBLE ENDOR.

Details see text.

two NMR transitions. Thus, when modulating the two NMR transitions with different frequencies and using a double lock-in technique, one can for instance induce one particular ENDOR transition of a particular neighbor nucleus and monitor the change of the ENDOR signal height as a function of a simultaneous second ENDOR transition. One observes changes of the ENDOR line intensity as a function of the second frequency swept rf source. A change is observed when a second ENDOR transition is induced at a nucleus, which is also coupled to the same electron, but not, if the nucleus belongs to a different center. The ESR of this different center may also be saturated if the ESR spectra of the different centers overlap (see Fig. 6). Therefore, this triple resonance experiment can be used to separate the ENDOR spectra of different paramagnetic centers if their ESR spectra overlap. Such a separation may well be impossible otherwise if the centers have many ENDOR lines with complicated angular dependencies. An example for such an experiment is shown in Fig. 7 for two types of F centers in BaFCl. The unpaired electron can either replace a Cl^- or an F^- ion and it is not possible to produce $F(F^-)$ centers without the simultaneous production of $F(Cl^-)$ centers[12]. Both ESR spectra overlap strongly and the ENDOR spectra of higher shell neighbors are not separable

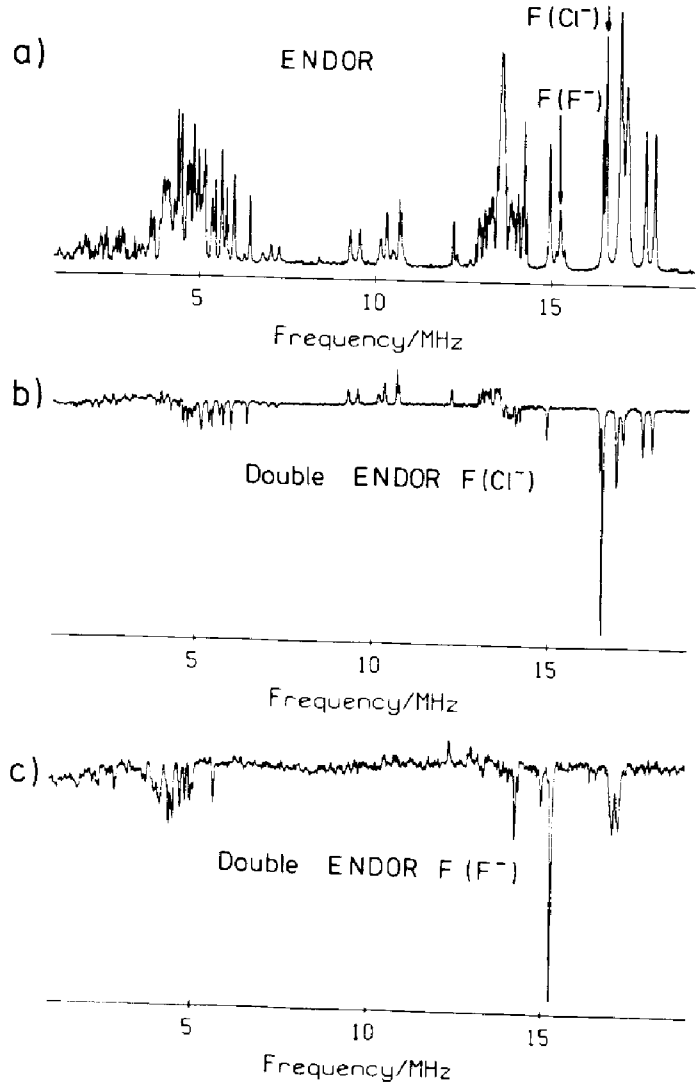

FIGURE 7 a) Part of the ENDOR spectrum of $F(Cl^-)$ and $F(F^-)$ centers in BaFCl.
b) DOUBLE ENDOR spectrum of the spectrum of Fig. 7a due to $F(Cl^-)$ centers.
c) DOUBLE ENDOR spectrum of the spectrum of Fig. 7a due to $F(F^-)$ centers.
All 3 Figures after (13).

from an analysis alone. Fig. 7a shows part of the ENDOR spectrum with lines of both centers. Fig. 7b is the spectrum obtained for setting the one ENDOR frequency to a line of $F(Cl^-)$ centers and Fig. 7c is the corresponding DOUBLE ENDOR spectrum for setting one frequency to a line of the $F(F^-)$ center. The spectra of both

centers are now separated. The fact that positive and negative signals occur, is understood[13]. The technique can also be used to investigate low symmetry defects, which otherwise can only be analysed in favourable circumstances. A recent example is the investigation of O^- centers in α-Al_2O_3, where the center has no symmetry anymore. An assignment of ENDOR lines to a particular center orientation was not possible without such triple resonance experiments[14,15].

4. OPTICALLY DETECTED ELECTRON SPIN RESONANCE (ENDOR)

Optical detection of electron spin resonance is a method long known in color center physics. It was mainly used for the study of optically excited states. Primarily the microwave-induced change of the magnetic circular dichroism (MCD) of the optical absorption was used to detect the ESR spectra of ground and excited states, e.g. for the F center[16]. The method is based on the fact that the MCD is proportional to the spin polarisation of the Zeeman levels, which can be diminished by saturating an ESR transition. Thus, upon fulfilling the resonance condition, the MCD decreases. The decrease of the MCD is monitored as ESR signal. This is shwon schematically in Fig. 8 for the ESR of the ground state.

Recently this method of measuring the spectrum of the ground state was applied to solve a different kind of problem. It is to correlate directly the optical and structure properties of a paramagnetic defect. Such problems arise mainly when studying defects created by radiation damage, since then usually many defects are created simultaneously, and it is very hard if not impossible to correlate optical properties like absorption or emission bands with specific ESR spectra, which could give information about the defect structure if hf or shf interactions are resolved. Such a case of recent interest was the study of Tl^+ doped alkali halides, where laseractive Tl related color centers

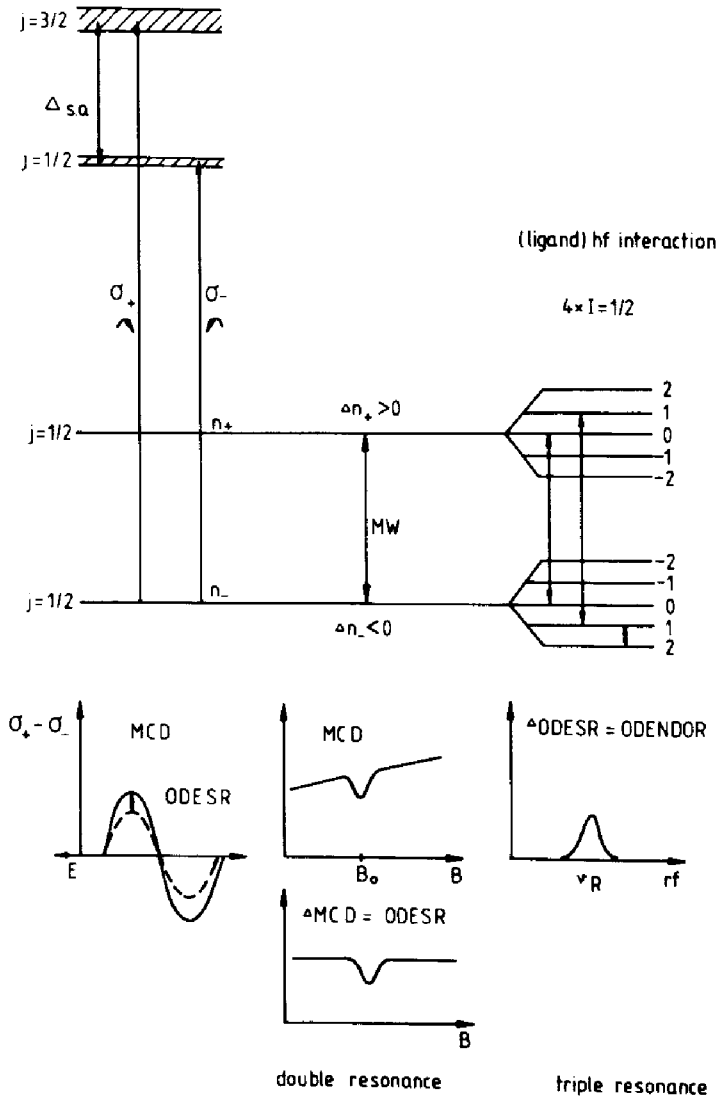

FIGURE 8

Schematical representation of the ODESR and ODENDOR mechanism when monitoring the microwave and rf induced change of the magnetic circular dichroism (MCD) of the absorption. Details see text.

could be produced by ionizing radiation[17]. By measuring the ODESR spectrum using the MCD of the near infrared absorption band at 1040 nm it could be shown that the laseractive center is identical with the center previously characterized by conventional ESR as being a $Tl^0(1)$ center, in which a Tl^0 atom resides next to an anion vacancy[18]. Fig. 9 shows the ODESR spectrum in a highly doped (2 mol%) KCl:Tl crystal. The large doublet splitting is due to the hf interaction with the central Tl nucleus (I = 1/2). It is seen for centers with their axes parallel and perpendicular to the magnetic field. The small doublets in between are forbidden transitions (for details see (19)). In order to identify all

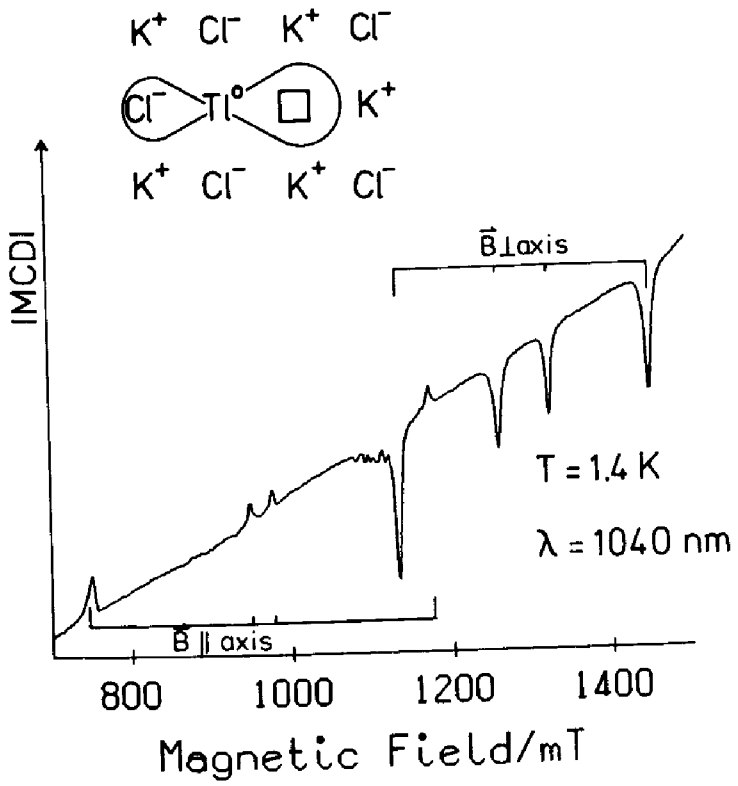

FIGURE 9

ODESR spectrum of $Tl^{o}(1)$ centers in KCl measured at 1040 nm at 1.4 K for $B_o \| [100]$. $\nu \approx 24$ GHz. After (9).

absorption transitions from the $Tl^{o}(1)$ centers within the total absorption of the crystal, which is the result of a superposition of the absorption bands of many defect species, another technique was developed, which was coinced as "MCD tagged by ESR" (19). In this technique one selects one particular ODESR transition, e.g. a Tl doublet line of the perpendicular centers, and varies the optical wavelength while monitoring the change of the MCD signal under resonance conditions. Thus, from the total MCD one measures only that part, which belongs to the particular ESR signal and center, repectively. In this way the optical absorption bands of a particular center - in this case center orientation - are selected out from the total absorption. Fig. 10a shows this for the $Tl^{o}(1)$ centers with their axes perpendicular to the magnetic field.

In Fig. 9 at about 1.1 T an additional ESR spectrum is weakly seen, which can be measured also at approximately 1040 nm and which belongs to a different defect. Its ESR spectrum is entirely differ-

ent from that of the $Tl^{o}(1)$ center. It appears especially in samples highly doped with Tl[19]. Fig. 10b shows its MCD tagged by ESR for B_o perpendicular to the center plane, which is strikingly similar to that of $Tl^{o}(1)$ centers. Both centers must be closely related. The drawback of this similarity is, of course, that the presence of this additional center will impair the laser properties of a $Tl^{o}(1)$ laser crystal. Fig. 11 shows the angular dependence

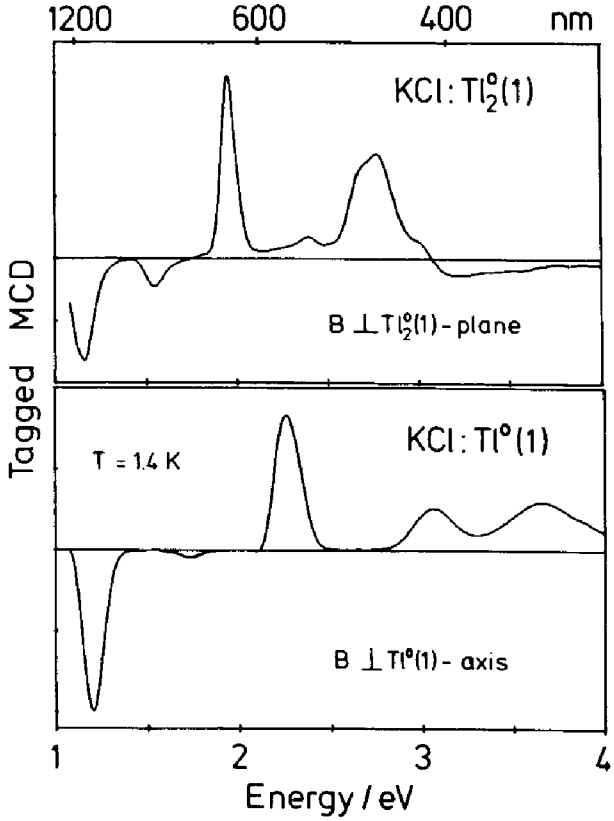

FIGURE 10

a) MCD tagged by ESR of $Tl^{o}(1)$ centers in KCl. B_o to center axis. After (19).

b) MCD tagged by ESR of $Tl_2^o(1)$ in KCl, B_o to center plane.

of the ESR lines of this center measured at 830 nm and for rotation of B_o in a (100) plane. The analysis yields the center model of Fig. 12: the unpaired electron is shared by two Tl^{+} ions and one anion vacancy. Table 2 compares the Tl hf constants and the g-values of both centers[20].

The method of measuring the ground state ESR via the microwave induced change of the MCD has the important advantage of high sensitivity and high selectivity. Compared to conventional

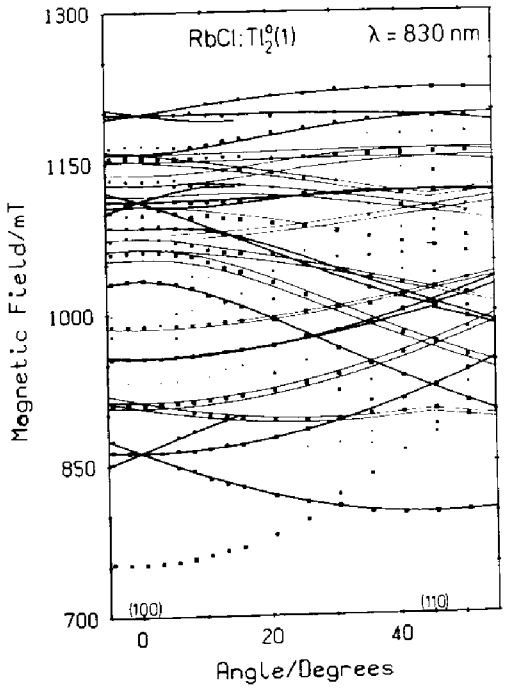

FIGURE 11 Angular dependence of the ODESR spectrum of $Tl_2^o(1)$ centers in KCl for rotation of B_o in a (100) plane. λ = 830 nm.

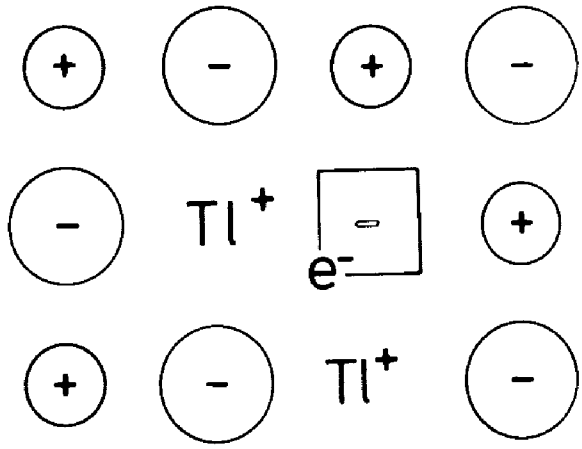

FIGURE 12 Model of the $Tl_2^o(1)$ center.

TABLE 2 Isotropic and anisotropic Tl hf interaction constants and g-factors of $Tl^{o}(1)$ and $Tl_2^{o}(1)$ centers in KCl

$Tl^{o}(1)$	$Tl_2^{o}(1)$
a = -10 mT	a = 71 mT
b = 191 mT	b = 85 mT
$g_{\parallel}$ = 1.7892	g_{011} = 1.711
$g_{\perp}$ = 1.3077	$g_{01\bar{1}}$ = 1.626
	g_{100} = 1.539

ESR, where all paramagnetic centers are measured simultaneously, in this method one particular center species can be singled out via one absorption band and investigated separately. This is a great advantage if angular dependencies are complicated (see Fig. 11!). Furthermore, the method proves a direct unambiguous experimental correlation between optical and structure properties, which otherwise cannot be obtained.

Fig. 13 shows the ODESR spectrum of the first relaxed excited state of the $Tl^{o}(1)$ centers for several field orientations measured via the microwave induced change of the magnetic circular dichroism of the emission (MCPE). The "sharp" peaks are the ground state resonances. The spectrum is extremely broad. The reason for this is not yet fully understood. It probably is due to the localised Tl motions[21].

5. OPTICALLY DETECTED ENDOR (ODENDOR)

Although with ENDOR a high resolution of shf interactions can be achieved, the method suffers from the drawback, that the ENDOR effect observed in solid state defects usually is only atmost of the order of a few percent of the ESR effect. Thus, correspondingly high center concentrations are needed. Therefore, the application

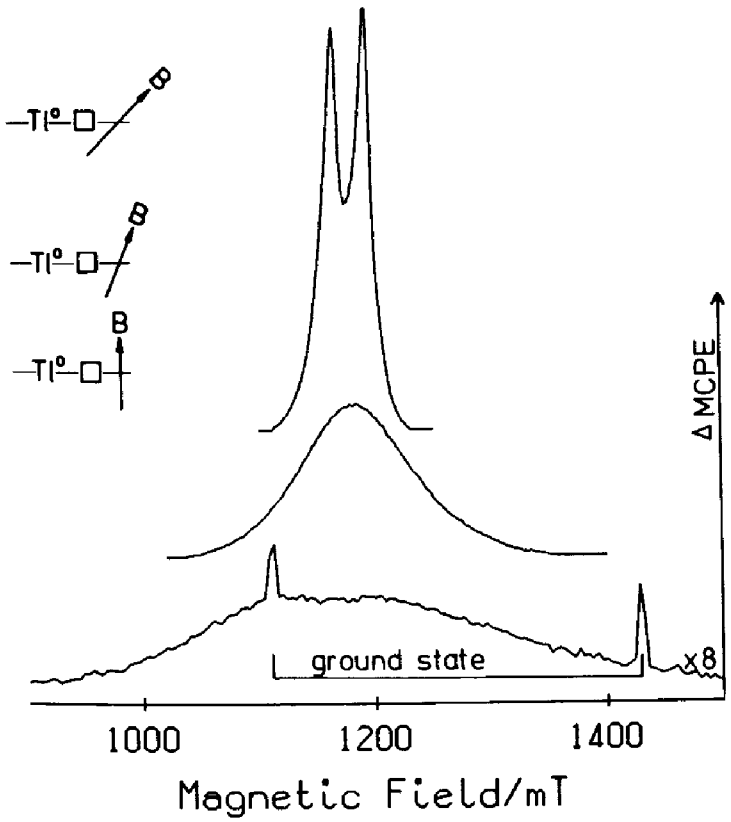

FIGURE 13

ODESR spectrum of the relaxed excited state of $Tl^{o}(1)$ centers in KCl for several B_o orientations. $T = 1.4$ K. The spectra were measured as microwave induced changes in the emission (MCPE).

of optical detection has the advantage of higher sensitivity, in principle by several orders of magnitude. So, the high selectivity of the optical detection promises additional advantages, provided the defect under study possesses an optical band and a spin orbit effect in the excited states large enough to give an appreciable MCD effect.

Recently, we could measure with optically detected ENDOR a defect ground state in which the shf interactions could be resolved. The idea of the experiment is schematically shown in Fig. 8. In an ODESR transition only particular nuclear spin states are selected by the microwave giving rise to a decrease of the MCD of the absorption. Thus, the total MCD decrease possible if all nuclear sublevels were involved is not achieved. Therefore, if simultaneously rf transitions between the nuclear sublevels are induced, additional spin packets are shifted into the microwave transition and therefore the decrease of the MCD is enhanced.

This effect was indeed observed. The ENDOR mechanism here is different from conventional ENDOR. The ENDOR signals can be of the same order as the ODESR signals, which was indeed observed. Therefore, this method is particularly useful for low center concentrations and samples with many species of defects because of the high selectivity. The method was applied to the socalled antisite defects in semi-insulating GaAs, in which a Ga atom is replaced by an As atom forming a paramagnetic $AsAs_4$ donor complex.

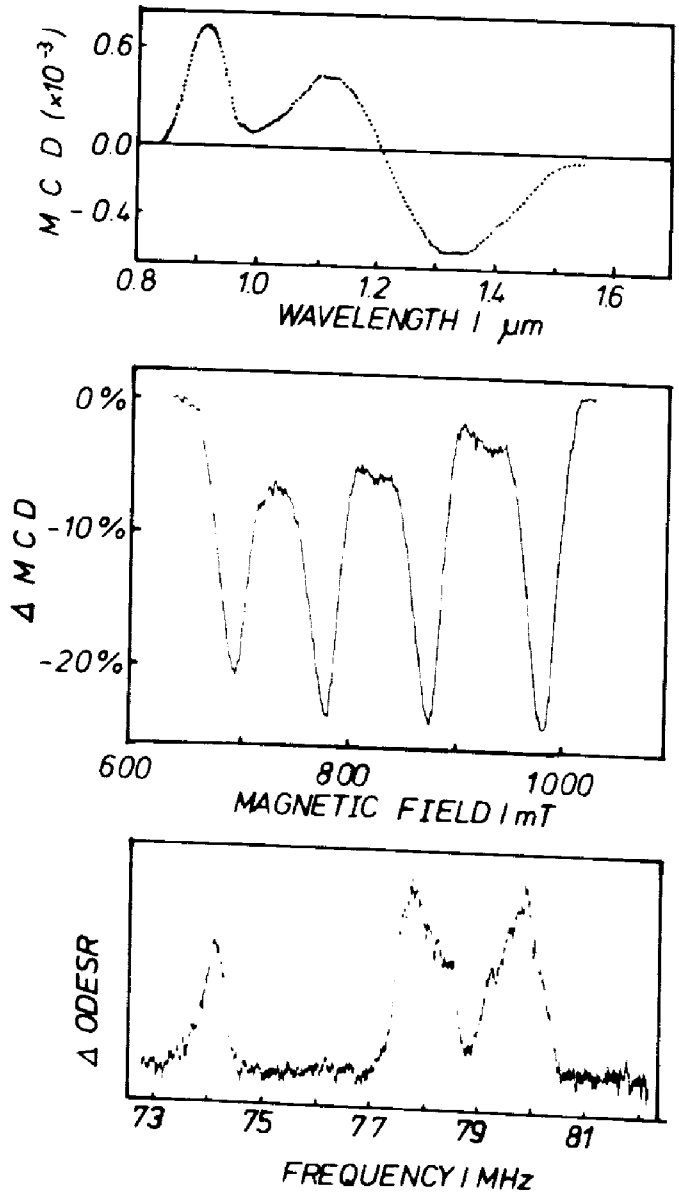

FIGURE 14

a) Magnetic circular dichroism of the As_{Ga} antisite defect in s.i. GaAs:Cr. After (22)

b) ODESR spectrum of the As_{Ga} antisite defect in s.i. GaAs:Cr. After (22).

c) Part of the ODENDOR spectrum of the As_{Ga} antisite defect in s.i. GaAs:Cr for B_o 3° off [110]. T = 1.6 K, ν = 24.1 GHz, λ = 1320 nm. After (23).

Fig. 14a shows the MCD, Fig. 14b the ODESR spectrum, in which the hf interactions with the central As nucleus (I = 3/2) is resolved[22]. Fig. 14c shows part of the ENDOR spectrum of the nearest As neighbors in a semi-insulating GaAs:Cr sample. It contains fully symmetric and distorted antisite defects[23].

6. CONCLUSION

Multiple resonance techniques proved to be very powerful tools for determining the structure of point defects also in difficult circumstances like the simultaneous presence of many defects or in systems where the resonances are very broad or where there are low concentrations. Their application to the study of ground states of defects can be an invaluable contribution to the field of material science. Technically, the availability of microcomputers and lasers facilitates greatly their use. Potentially, the optical technique can also be used to study the spatial distribution of defects and defects in thin layers, an area, which is of increasing importance in semiconductor physics.

Acknowlegements - The authors would like to thank Dr. J.R. Niklas, Dr. F. Lohse, Dr. B.K. Meyer, Mr. F.J. Ahlers and Mr. P. Studzinski for many helpful discussions.

REFERENCES

1. G. Feher, Phys. Rev. 105, 1122 (1957)
2. H. Seidel, Z. Physik 165, 218 (1961)
3. H. Seidel and H.C. Wolf in "Physics of Color Centers", ed. by W.B. Fowler, Acad. Press 1968, N.Y., Chapter 8
4. Y. Ueda, J.R. Niklas, J.-M. Spaeth, U. Kaufmann and J. Schneider, Solid State Comm. 46, 127 (1983)
5. J.R. Niklas and J.-M. Spaeth, to be published
6. J. Casas-Gonzáles, A.W. den Hartog and R. Alcalá, Phys. Rev. B.21, 3826 (1980)
7. P. Studzinski, J. Casas-Gonzáles and J.-M. Spaeth, J. Phys. C: Solid State Physics 17, 5411 (1984)

8. D.S. Pan and F. Lüty, Phys. Rev. B18, 1868 (1978)
9. P. Fuhrberg, Diplomarbeit Hannover 1983
10. H. Söthe, Diplomarbeit Paderborn 1984
11. H. Söthe, P. Studzinski and J.-M. Spaeth, to be published
12. R.U. Bauer, J.R. Niklas and J.-M. Spaeth, phys. stat. sol. (b) 118, 557 (1983)
13. R.U. Bauer, J.R. Niklas and J.-M. Spaeth, phys. stat. sol. (b) 119, 171 (1983)
14. J.R. Niklas, R.C. DuVarney and J.-M. Spaeth, Intern. Conf. on Defects in Insulating Crystals, Salt Lake City, 1984, abstracts p. 341
15. R.C. DuVarney, J.R. Niklas and J.-M. Spaeth, phys. stat. sol., to be published
16. L.F. Mollenauer, S. Pan and S. Yngvesson, Phys. Rev. Lett. 23, 689 (1969)
17. W. Gellermann, F. Lüty and C.R. Pollack, Opt. Commun. 39, 391 (1981)
18. E. Goovaerts, J.A. Andriessen, S.V. Nistor and D. Schoemaker, Phys. Rev. B24, 29 (1981)
19. F.J. Ahlers, F. Lohse, J.-M. Spaeth and L.F. Mollenauer, Phys. Rev. B28, 1249 (1983)
20. F.J. Ahlers, F. Lohse and J.-M. Spaeth, to be published
21. M. Fockele, F.J. Ahlers, F. Lohse, J.-M. Spaeth and R.H. Bartram, J. Phys. C:Solid State Physics 1984, in press
22. B.K. Meyer, J.-M. Spaeth and M. Scheffler, Phys. Rev. Lett. 52, 851 (1984)
23. D.M. Hofmann, B.K. Meyer, F. Lohse and J.-M. Spaeth, Phys. Rev. Lett. 53, 1187 (1984)